QMENTA®

Unraveling Parkinson's: The Power of Neuroimaging Biomarkers

Whitepaper

Unraveling Parkinson's: The Power of Neuroimaging Biomarkers

Introduction

Parkinson's Disease (PD) has emerged as the second most prevalent neurodegenerative disorder, impacting up to 3% of individuals aged 65 and older (Poewe et al., 2017). In a world with an aging population, its increased prevalence is going to represent a major challenge for healthcare systems.

PD is characterized by neuronal loss in the substantia nigra producing the following cardinal manifestations: bradykinesia, tremors, rigidity and postural instability (Postuma et al., 2015). Their origin is based on the progressive deterioration of dopaminergic neurons within the substantia nigra pars compacta (SNpc) (Kalia & Lang, 2015). However, long before these motor symptoms emerge, PD patients often experience a range of prodromal symptoms, including rapid eye movement sleep behavior disorder, constipation, and hyposmia (impaired sense of smell). These non-motor symptoms can appear years before motor dysfunction, indicating that PD begins its pathological course long before its classical features become evident (Figure 1; Poewe et al., 2017).

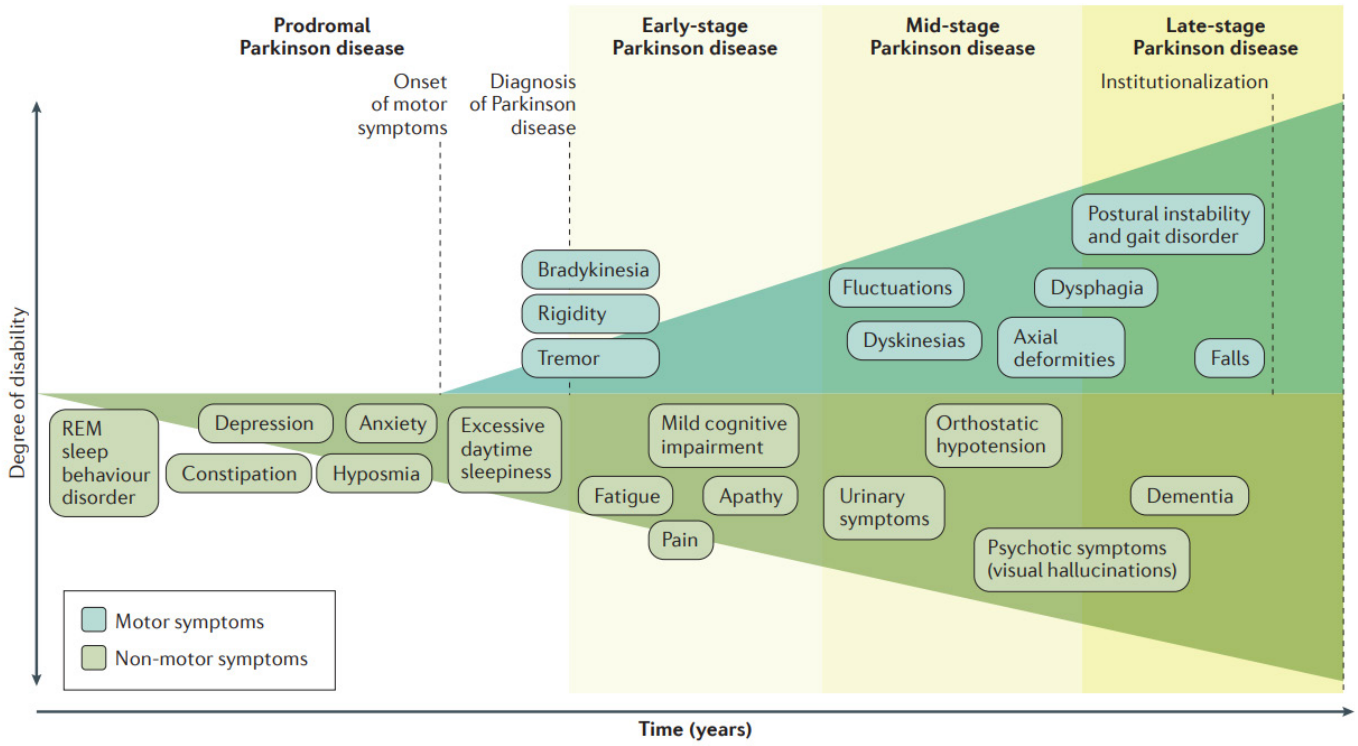

Figure 1. Motor and Non-Motor Symptoms in Parkinson's Disease: The onset of motor symptoms in Parkinson's Disease marks the point of diagnosis. However, these motor symptoms are often preceded by a prodromal phase lasting years or even decades, characterized by specific non-motor symptoms. Adapted from Poewe et al. (2017).

The diagnosis of PD is typically prompted by the emergence of motor symptoms. Initially, the patient's clinical history is reviewed to identify prodromal symptoms (e.g., rapid eye movement, sleep behavior disorder, hyposmia, constipation), characteristic movement difficulties (e.g., tremor,

stiffness, slowness), and cognitive issues (e.g., cognitive decline, depression, anxiety). Its diagnosis has two main examinations, the psychological and the neurological. The psychological examination is based on several psychological and motor tests. The main motor test for diagnosis is the Movement Disorders Society Unified Parkinson's Disease Rating Scale III (MDS-UPDRS III) (Goetz et al., 2008) which is evaluating the signs of bradykinesia, tremor and rigidity (Postuma et al., 2015). Additionally, scales like the Hoehn and Yahr (H&Y) focus on the degree of clinical disability produced by the symptoms (Hoehn & Yahr, 1967). There is also a progressive cognitive deterioration that is evaluated initially by the Montreal Cognitive Assessment (MoCA) (Nasreddine et al., 2005). In the long term, this cognitive impairment requires more specific evaluation by assessing each cognitive domain separately (Attention & working memory, executive function, language, memory and visuospatial abilities) (Litvan et al., 2012).

Although the psychological and motor tests can narrow the diagnosis, there are several atypical parkinsonian syndromes, including Multiple System Atrophy (MSA), Progressive Supranuclear Palsy (PSP), and Corticobasal Degeneration (CBD), which share similar motor symptoms but have distinct underlying pathologies. Differential diagnosis between PD and these atypical forms of parkinsonism is essential, as they vary significantly in disease progression, response to treatment, and prognosis. Early and accurate diagnosis is critical to improve patient outcomes and tailor treatment strategies.

During recent decades, neuroimaging techniques have become invaluable tools in the differential diagnosis and early detection of PD. These imaging modalities help distinguish PD from other neurodegenerative disorders by providing insights into structural, functional, and metabolic changes in the brain. Current state-of-the-art imaging techniques include dopamine transporter PET (DAT-PET) and single-photon emission computed tomography (DAT-SPECT). DAT-PET was first proposed to assess the dopaminergic dysfunction in the brain – it was presented in 1980 (Garnett et al., 1983). Later on, DAT-SPECT appeared as an affordable and less radioactive technique than DAT-PET for the same purpose. Both DAT-SPECT and DAT-PET are currently largely employed to differentiate patients with parkinsonian syndromes (PD, MSA, PSP, CBD) from those with essential tremor and healthy controls (HC) (Politis, 2014). Albeit the DAT-PET worldwide usage, over the past 25 years there has been little improvement towards the differential diagnosis of these movement disorders syndromes. In the early stages of PD, the response to dopaminergic treatment is less evident, and distinguishing symptoms of alternative diagnoses, such as MSA, may not yet be evident.

MRI is highly valued for its ability to provide exceptional soft tissue contrast without the use of ionizing radiation, making it a safe and non-invasive tool for repeated imaging. Its versatility allows for detailed anatomical and functional imaging, offering comprehensive insights into brain structure and activity. Additionally, MRI provides unique insights into both the structural and functional changes in the brain to understand the early phases and progression of the disease. Advanced MRI techniques, such as Voxel-Based Morphometry (VBM), Quantitative Susceptibility Mapping (QSM), and Diffusion Tensor Imaging (DTI), allow for the detection of key biomarkers like iron accumulation in the substantia nigra, brain atrophy, and microstructural white matter changes, all of which are early indicators of PD. These techniques can differentiate PD from other neurodegenerative disorders, such as MSA and PSP, improving diagnostic accuracy. Furthermore, MRI's ability to track changes in brain morphology and function over time offers valuable insights into disease progression and helps tailor treatment strategies, making it an essential tool in both research and clinical practice for understanding PD. Functional MRI (fMRI) is also employed to study the neural bases of cognitive deficits and assess functional connectivity changes in PD patients.

Next, we will show the key findings from decades of research utilizing neuroimaging techniques such as MRI, PET, and SPECT.

Structural Imaging Insights in Parkinson's Disease

Conventional MRI encompasses the acquisitions that rely on contrast differences between tissues. These images are captured using various combinations of contrasts, each resulting in a distinct type of weighted image. In PD, the most representative acquisition is T1-weighted MRI (T1w). T1-weighted MRI structural acquisition focuses on examining brain morphometry. Researchers have employed T1w to investigate global or regional brain structure and also longitudinal changes. It has also been applied for differential diagnosis of PD from MSA or PSP.

A common analysis consists of Voxel-based morphometry (VBM) which estimates group differences in the density or volume across the entire brain with a high regional specificity (Ashburner & Friston, 2000). For differential diagnosis, VBM has demonstrated the ability to distinguish PSP and MSA from PD and HC with 74–83% sensitivity and 79–94% specificity, based on the detection of atrophy in the cerebral peduncles of patients with PSP (Paviour et al., 2005; Price et al., 2004). Longitudinal studies in PD patients using VBM have documented increased regional atrophy in key brain regions, such as the hippocampus, occipital fusiform gyrus, and precuneus (Gee et al., 2017; Ibarretxe-Bilbao et al., 2010). However, VBM analyses comparing early-stage PD patients and HC did not reveal significant differences in the rates of regional gray matter (GM) volume loss over a period of up to three years (Yang et al., 2018; Zeng et al., 2017). Earlier findings point out that whole-brain VBM analysis may lack the sensitivity to detect differing rates of regional brain alterations between PD patients and matched HC. However, it still proves effective for the differential diagnosis of PD from PSP and MSA.

Similarly to VBM, Tensor-based morphometry (TBM) is a different voxel-wise structural analysis technique that extracts structural differences from the gradients of deformation fields that warp images to a common anatomical template (Ashburner & Friston, 2000). Applying this technique to 22 PD patients, Tessa et al 2014 found significantly higher yearly atrophy rates in the prefrontal cortex, anterior cingulum, caudate, and thalamus in PD patients compared to HC over 3 years in the early stages of the disease (Tessa et al., 2014). These findings highlight that cortical and subcortical regions related to cognitive functions show progressive atrophy detectable in the early stages of the disease.

Structural MRI can be further exploited by measuring cortical thickness (Fischl & Dale, 2000). This approach has also gained traction identifying the specific patterns of cortical degeneration that characterizes PD. Some studies showed that early stage PD subjects significantly decreased their cortical thickness than HC in the left occipital and bilateral frontal lobes, right motor-sensory cortex and the left caudal middle frontal cortex over a year (Yau et al., 2018). However, these results are not conclusive since other cortical thinning studies did not find significant differences between PD and control groups (Campabadal et al., 2017; Garcia-Diaz et al., 2018). These discrepancies might be due to the clinical heterogeneity in PD patients. Specifically, PD patients with mild cognitive impairment (MCI) (compared to HC and cognitively normal PD) exhibit more extensive atrophy and faster cortical thinning in the frontal and temporoparietal cortices, including hippocampal atrophy, over 18 months (Mak et al., 2015). These findings indicate that structural changes detected by these methods are more prevalent in PD subgroups with additional cognitive symptoms. Moreover, the

results can be influenced by the measurement used to quantify cortical thickness (average change, temporal average, percent change, symmetrized percent change or annual rate of cortical thickness change). Despite these discrepancies, substantial evidence indicates that in early and moderate stages of PD, subjects present accelerated total GM loss and frontal cortical thinning compared to HC (Ibarretxe-Bilbao et al., 2010; Mak et al., 2015; Nürnberger et al., 2017; Yau et al., 2018). As expected, PD patients with MCI have accused atrophy and faster rates of cortical thinning in frontal and temporoparietal cortices and the hippocampus over 18 months compared to cognitive normal PDs (Hanganu et al., 2014; Mak et al., 2015).

In summary, T1-weighted MRI structural acquisitions are essential to study brain morphometry and to differentiate PD from other disorders like MSA and PSP. Techniques like VBM and TBM have shown effectiveness in detecting brain atrophy and structural differences in PD patients. Cortical thickness measurements also highlight PD-related cortical degeneration, though results can vary due to clinical heterogeneity.

Quantitative measurements approaches

Quantitative MRI (qMRI) is an emerging field that instead of focusing on the contrast of weighted images, provides quantitative information on the underlying physiological properties of tissues. A great example are relaxation times which can be used as a proxy of the neuromelanin content. In fact, imaging of the substantia nigra (SN) plays an important role in PD diagnosis and prognosis. However, SN's limited size and low contrast in standard T1-w sequence hinders SN segmentation, and hence, the evaluation of atrophy (Lehericy et al., 2017). To counteract this, novel MRI acquisitions sensitive to neuromelanin and iron provide a different measure of physiological changes in the SN.

T2 relaxation time acquisitions

Neuromelanin and Iron influence the T2* relaxation times in different ways. In MRI physics T2 is defined as a time constant for the decay of transverse magnetization that results from natural interactions at the atomic or molecular levels. However, in real experiments the transverse magnetization decays much faster than would be predicted by natural atomic and molecular mechanisms, this faster decay is denoted as T2*. T2* results principally from inhomogeneities in the main magnetic field. Iron can provoke changes in the local magnetic susceptibility and thus shortens T2* relaxation times of nearby water protons (Dusek et al., 2013). Meanwhile, in the space between adjacent myelin membrane layers, water protons frequently interact with non-aqueous components. This interaction speeds up transverse and longitudinal relaxation and causes magnetization exchange between water and macromolecular protons, known as magnetization transfer (Möller et al., 2019). Therefore, specialized T2* relaxation acquisitions can focus on measuring these distinctive effects allowing neuromelanin and Iron sensitive imaging.

In neuromelanin imaging, research studies have shown that normalized neuromelanin volume of the anterior, posterior, and whole SN correlated with PD severity. Additionally, the SNpc neuromelanin sensitive area correlated with motor impairment and disease duration (Schwarz et al., 2017; Taniguchi et al., 2018). Moreover, motor asymmetry in PD is reflected in the contralateral SN volume reduction and signal decrease (Prasad et al., 2018). Despite these contributions, differential diagnosis of PD from HC is not possible based on neuromelanin imaging alone since neuromelanin content also decreases in HC after the age of 50 (Xing et al., 2018).

Meanwhile, Iron sensitive MRI studies focus on the Dorsal Nigral Hyperintensity (DNH; Figure 2), an area characterized by a contrast of iron-poor hyperintense nigrosome-1, surrounded by iron-rich and hypointense SN. In PD, this hypersignal of the DNH is reduced or lost bilaterally compared to control subjects (Mahlknecht et al., 2017; Schwarz et al., 2014). However, the detection of DNH loss for PD diagnosis has limitations, even at ultra-high-field (7T), there are 10% of false negative scans and it still depends on experienced raters (Mahlknecht et al., 2017). Moreover, DNH can also not be visible (Schmidt et al., 2017) or be asymmetric (Gramsch et al., 2017) in 15 to 25% of healthy subjects due to the proximity of micro-vessels and the superior cerebellar artery causing pulsations artifacts (Kau et al., 2019).

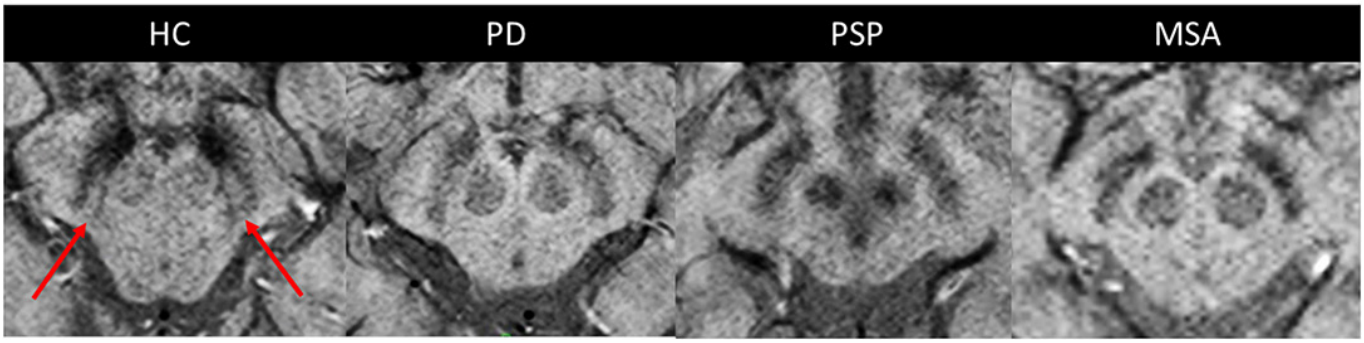

Figure 2. Dorsolateral nigral hyperintensity (DNH). As indicated with the arrows DNH is well-depicted at the dorsolateral part of the substantia nigra pars compacta in a healthy control. DNH is lost in Parkinsonian syndromes, such as PD, PSP and MSA. Adapted from Chougar et al., 2020.

Although neuromelanin and iron sensitive acquisitions have helped to understand the disease, the relaxometry rates are influenced by changes in water content, local water diffusion rates in an inhomogeneous field and macroscopic magnetic field inhomogeneities (Barbosa et al., 2015). Nevertheless, these problems have been approached by other qMRI sequences such as Quantitative susceptibility mapping or free-water diffusion MRI.

Quantitative susceptibility mapping

Techniques such as iron sensitivity T2 relaxation depends on the tissue shape and orientation and is susceptible to artifacts from the dipole field, making this acquisition an indirect measurement of iron concentration. These problems are addressed by Quantitative susceptibility mapping (QSM; Figure 3), which maps the local susceptibility sources underlying the measured field using the dipole kernel field deconvolution (Liu et al., 2009). Iron overload in SN measured by QSM is the most studied and utilized MRI biomarker for PD (X. Guan et al., 2024). At the time of diagnosis, significant iron deposition in SN was detected by QSM with higher sensitivity compared to R2* mapping (Barbosa et al., 2015; Du et al., 2016). Additionally, further research has confirmed the relationship between asymmetrical nigral iron deposition and motor laterality (Azuma et al., 2016). Studies with QSM have also confirmed a correlation between dentate iron deposition and parkinsonian tremor (He et al., 2017; Zhang et al., 2023), as well as between mild cognitive impairment and cerebral/subcortical iron burden (Kang et al., 2022; Thomas et al., 2020).

Figure 3: QSM axial section at the basal ganglia level in a PD patient. Segmentation highlights the caudate nucleus, putamen, and globus pallidus highlighted in red, green, and blue, respectively. Adapted from Azuma et al., 2016.

Longitudinal studies have observed changes in iron deposition in the SN of PD patients. Du et al. 2018 found increased iron in the SNpc and decreased iron in the SN reticulata over 18 months. Overall, SN iron content shows significant increases after 36 months (Bergsland et al., 2019). However, Thomas et al. 2024 did not observe significant regional changes over three years. These studies, though limited by small sample sizes, suggest that iron metabolism in the SN during PD progression may be complex and variable, necessitating further research to clarify these dynamics.

Several clinical tests have sought to identify iron-related biomarkers for diagnosing PD with promising performance. Studies using ROC analysis reported AUCs of 0.70–0.91 for classifying PD patients from HC via QSM values in the SN (Barbosa et al., 2015; Takahashi et al., 2018; Zhang et al., 2022). A multimodal approach combining QSM with other MRI modalities, based on 36 features where SN magnetic susceptibility was crucial, achieved diagnostic accuracies of 81.1% in internal testing and 78.5% in external validation (X.-J. Guan et al., 2022). Future research should focus on advanced big-data technology, larger sample sizes, and multi-center collaboration to enhance clinical translation of these methods.

Diffusion weighted imaging

Another branch of quantitative-MRI is diffusion weighted MRI, a technique that samples the diffusivity of water molecules via diffusion weighting gradients. Hence, dMRI is sensitive to microstructural tissue changes that alter the regional diffusion of water molecules. Therefore, it is crucial in white matter (WM) characterization. Using diffusion tensor imaging (DTI), studies have reported reduced fractional anisotropy (FA) in the SN, though there is considerable variability in the results (Schwarz et al., 2013). A major limitation of DTI is that changes in fast-diffusing extracellular compartments can skew the estimation of DTI indices, complicating the interpretation of signal changes (Andica et al., 2019). Dealing with this issue, Free-water (FW) imaging employs a bi-tensor model from which a measure of diffusion fractional anisotropy within the tissue (FAt) can be calculated avoiding these skewness (Pasternak et al., 2009).

In PD, a longitudinal pattern of elevated free water in the SN relative to HC has been revealed by several studies. A recent validation study using the Parkinson Progression Marker Initiative Cohort corroborated these findings (Burciu et al., 2017), showing that: (1) free water levels in the posterior

SN increased over one year in de novo PD but not in HC; (2) free water levels continued to rise over four years in PD; (3) sex and baseline free water levels predicted four-year changes in free water; (4) increases in free water over one and two years were related to worsening on the Hoehn and Yahr (H&Y) scale over four years; and (5) the four-year increase in free water was associated with a decrease in striatal binding ratio in the putamen. Moreover, free-water can be a predictor of cognitive impairment in PD. Using the same dataset Guttuso and colleagues found that the Thalamic dorsomedial nuclei FW changes over 1 year correlated with the Montreal cognitive assessment changes over both 1 and 3 years (Guttuso Jr et al., 2022). Pointing out the dorsomedial nuclei of the thalamus as a progression biomarker in early PD.

Neurite Orientation Dispersion and Density Imaging (NODDI), assumes that water molecules in the brain are distributed across three distinct compartments: the intracellular compartment, the extracellular compartment, and the cerebrospinal fluid (CSF) compartment. This method estimates the microstructure of dendrites and axons by quantifying neurite density (NDI, indexed by intracellular volume fraction [ICVF]), orientation dispersion index (ODI), and isotropic volume fraction (ISOVF). In PD patients with neurocognitive and psychiatric disorders, ICVF is reduced in WM compared to those without these symptoms. Furthermore, ICVF significantly contributes to the diagnostic differentiation, indicating its potential as a biomarker for detecting microstructural changes in WM associated with psychiatric disorders in PD (Andica et al., 2020). Regarding WM microstructural alterations PD patients with levodopa-induced dyskinesia (LID) exhibit fewer WM microstructural changes, particularly in temporal lobe fibers, compared to PD patients without LID (Ogawa et al., 2021).

qMRI is an emerging field that provides specific physiological information, such as the relaxation times or diffusion-related coefficients, that help to extract information about the tissue microstructure. Advanced MRI techniques sensitive to neuromelanin and iron have shown correlations between these measures and PD severity, motor impairment, and disease duration. While neuromelanin decreases with age, complicating differential diagnosis, iron-sensitive MRI studies, including QSM, have identified iron overload as a significant biomarker for PD. DTI and FW imaging have revealed microstructural changes in the SN and WM, with FW levels correlating with PD progression and cognitive decline. NODDI further refines WM analysis by quantifying neurite density and orientation, with ICVF in PD patients linked to neurocognitive and psychiatric symptoms. These advanced imaging techniques highlight the potential of qMRI in improving PD diagnosis and understanding its progression.

Functional neuroimaging

Functional neuroimaging refers to a set of techniques used to measure brain activity by detecting changes associated with blood flow, metabolic processes, or neural activation. In this review we will focus on PET, SPECT which cover the metabolic processes imaging focusing on the differential diagnosis and fMRI which uses the BOLD signal as a proxy of neural activation to study cognitive function.

Molecular imaging

Molecular imaging techniques, such as PET or SPECT, involve measuring the decay of a radionuclide, during which a positron or γ-ray is emitted, producing photons. PET captures pairs of high-energy γ-rays emitted indirectly during the decay of radioisotopes like 11C, 13N, 15O, and 18F, which are introduced into the subject. The positrons released by these radioisotopes travel a few millimeters through the surrounding tissue, quickly losing their kinetic energy. As they slow down, they interact

with electrons, resulting in the production of γ-rays that travel in nearly opposite directions detected by PET detectors. Three-dimensional images of the body functional processes are then reconstructed through computer analysis. SPECT is based also in the capture of radioactivity, however SPECT radioisotopes emit a single γ-ray during decay that is measured directly by the scanner. Additionally, SPECT scans are considerably less expensive than PET scans, partly because the nuclides used in SPECT have longer half-lives and are easier to obtain than those used in PET.

In PD, PET has been used in differential diagnosis differentiating PD from parkinsonian syndromes such as PSP, MSA and corticobasal degeneration (CBD) using 18F-6-fluorodopa (L-3,4-dihydroxy-6-18F-fluorophenylalanine; 18F-DOPA) that tracks dopamine metabolism. PET studies showed an asymmetric loss of 18F-DOPA in the putamen with moderate preservation in the caudate whereas PSP had a symmetrical decrease of 18F-DOPA both in the putamen and the caudate nucleus (Golan et al., 2022). Distinguishing between MSA and PD is quite more difficult since in some MSA cases the 18F-DOPA uptake is reduced bilaterally similarly to late-stage PD (Thobois et al., 2019).

PET is also able to track glucose metabolism using the 8F-FDG tracer to differentiate PD from MSA and PSP (Figure 4). In fact, using network analysis several studies obtained a strong differentiation between PD (with 84–95% sensitivity and 94–97% specificity), MSA (85–96% sensitivity and 96–99% specificity), PSP (88–91% sensitivity and 94–99% specificity), and corticobasal degeneration (96% sensitivity and specificity) (Tang et al., 2010; Teune et al., 2013).

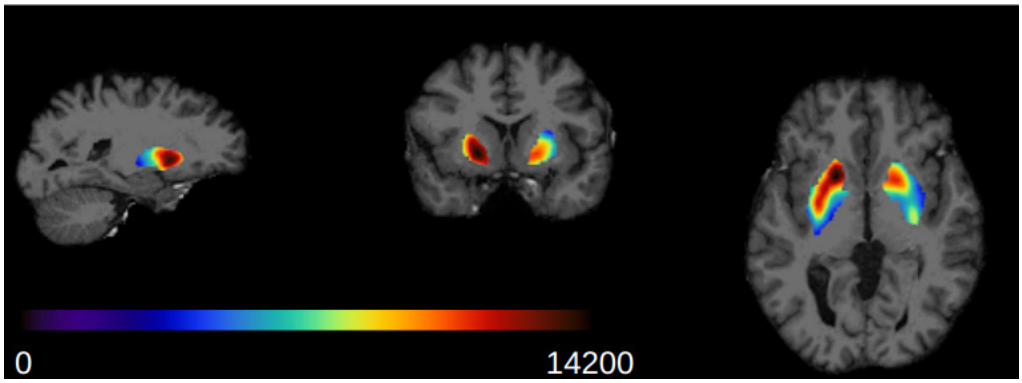

Figure 4. Parkinson disease putamen and pallidum 8F-FDG PET imaging. The background image corresponds to a MRI T1w structural of a Parkinson disease patient. The overlay is a 8F-FDG PET image only for the subcortical regions of the putamen and pallidum.

CBD is still one of the most difficult disorders to diagnose and to distinguish from PD. A first attempt to distinguish CBD from PD opened when Klaffke et al., 2006 proposed the use of DAT-SPECT, and 8F-FDG PET. The study concluded that glucose metabolism and DAT are reduced, while D2-receptors are frequently preserved in CBD, being insufficient for differential diagnosis. However, tau-PET tracers seem to be the most adequate choice since CBD is a tau pathology (Coakeley & Strafella, 2017). Second-generation tau PET tracers like [18F]PM-PBB3 or [18F]PI-2620 might be promising for CBD differential diagnosis (Mena & Strafella, 2022). However the gold standard is still Pathological diagnosis (Coakeley & Strafella, 2017; Mena & Strafella, 2022).

Complementing PET, DAT-SPECT demonstrates high sensitivity (87–98%) and specificity (80–100%) in distinguishing patients with parkinsonian syndromes (such as PD, MSA, PSP) from those with essential tremor and HC. In fact DAT-SPECT (DATSCANtm) is quite extended in clinical practice. Furthermore, the tracer 123I-Metaiodobenzylguanidine in SPECT or scintigraphy has been recommended for MSA and PD differential diagnosis when F-DOPA PET is not able to differentiate (Thobois et al., 2019).

Despite these advances there is not a clear PD molecular imaging protocol regarding differential diagnosis of PD from MSA, PSP and CBD. However, there have been proposals in the past. Nicastro

et al. suggested an imaging protocol based on a decision tree that included 18F-DOPA PET, 18F-FDG PET, 123I-MIBG SPECT or scintigraphy, and D2 PET (Figure 5; Nicastro et al., 2018).

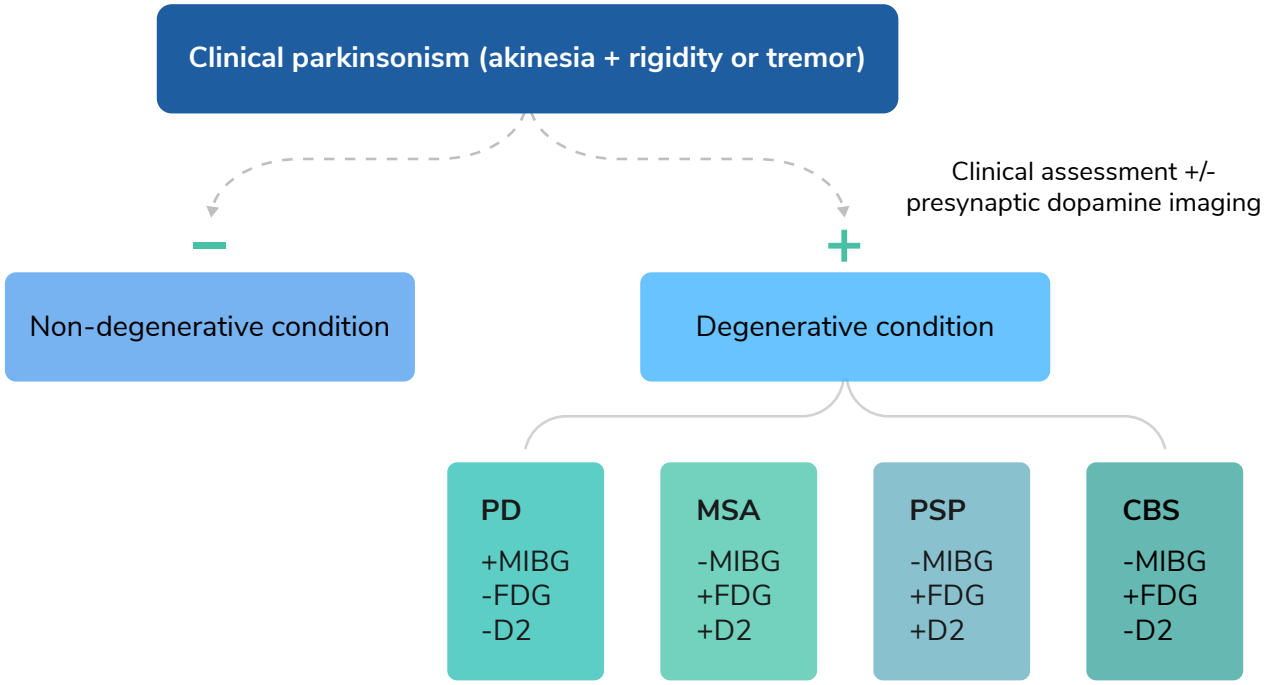

Figure 5. Proposed protocol in the evaluation of a subject with parkinsonism; (-) is normal and (+) pathological. CBS = corticobasalsyndrome; MSA = multiple system atrophy; PD = Parkinson's disease; PSP = progressive supranuclear palsy. Adapted from Nicastro et al., 2018.

Additionally DAT-SPECT could be incorporated to discard essential tremor cases. The first step is to identify degenerative and non-degenerative conditions using 18F-DOPA PET. Afterwards, 18F-FDG PET and 123I-MIBG scintigraphy will focus on identifying PD cases since 18F-FDG PET will be normal in PD and pathological in MSA, PSP and CBD whereas 123I-MIBG scintigraphy would be pathological in PD and normal in the rest of conditions. Finally, D2 PET will group PD and CBD as normal readings and MSA and PSP as pathological (Klaffke et al., 2006).

Functional MRI neuroimaging

fMRI was initially developed to detect task-related signal changes in the brain through BOLD contrast, and to explore functional connectivity across distant brain regions. These regions coordinate cortical and subcortical networks, which are identified through temporal associations of variations in the resting-state fMRI signal. PD research with fMRI has focused on studying the neural bases of cognitive deficits. In fact, altered connectivity within and between resting-state intrinsic connectivity networks have been related to different types of Parkinson's cognitive deficits.

First studies began pointing out the possible association between resting-state default mode network (DMN) connectivity and cognitive performance in PD. This was first suggested by Tessitore et al., (2012) in a study including a small sample of cognitively-normal PD patients and using independent component analysis. However, this connectivity seemed to be unchanged in PD patients with mild cognitive impairment (PD-MCI) compared to PD cognitively normal (PD-CN) (Amboni et al., 2015).

The sensorimotor network (SMN) is extensively studied in PD due to its critical role in motor degeneration and compensatory mechanisms. Early studies confirmed decreased functional connectivity in the SMN, dorsolateral prefrontal cortex (DLPFC), and putamen, which negatively

correlated with UPDRS-III scores, alongside increased cerebellar connectivity as a compensatory response in PD patients not on dopaminergic medication (Wu et al., 2009, 2011). Additionally, the SMN has been associated with executive function deficits (Lang et al., 2019).

The FPN is also affected by dopaminergic depletion of the cognitive-basal ganglia loop. In fact, The FPN has been related to both executive function deficits (Kehagia et al., 2012) and memory deficits (Lang et al., 2019).

These functional networks might partially help to understand MCI in PD patients. However, examining network interactions can further lead to a better understanding of PD-MCI. RSNs interaction can be studied by means of static resting-state FC, investigating connectivity among nodes that belong to different RSNs. In this vein, recent studies started looking at inter-network connectivity. Baggio et al., (2015) study went a step further and after group ICA analysis found reduced within-DAN, within-DMN and DAN-FPN connectivity associated with PD-MCI versus HC and PD-CN groups. The importance of frontal and temporal regions connectivity in PD-MCI is such that they have been used as biomarkers in classifiers (Abós et al., 2017). Another way of looking at between network connectivity is through dynamic functional connectivity at the synchronized activation of two RSN during the rs-fMRI recording. When looking at dynamic FC in PD-MCI Díez-Cirarda et al. 2018 found reduced FC mostly between SMN-FPN networks and graph-topological deteriorations in the SMN network for PD-MCI subjects. Despite these studies, RSN deterioration in PD-MCI depending on the cognitive profile is not completely understood. Therefore, the study of the interactions between networks connectivity might serve as a marker of PD-MCI and to foresee which functional connectivity interactions among networks might anticipate a more dysexecutive or posterior cortical centered MCI profile.

In Summary, we have seen how functional neuroimaging techniques, including PET, SPECT, and fMRI, play a crucial role in studying PD. PET, particularly with 18F-DOPA, helps distinguish PD from conditions like PSP and MSA by tracking dopamine metabolism, while 18F-FDG PET is effective in assessing glucose metabolism to differentiate PD with high sensitivity and specificity. DAT-SPECT is commonly used in clinical practice due to its high sensitivity and specificity in differentiating parkinsonian syndromes from essential tremor and HC. Despite advances, there is no standardized imaging protocol for differentiating PD from MSA, PSP, and CBD, though decision-tree-based protocols incorporating PET and SPECT have been proposed. fMRI is used to study neural activation and functional connectivity in PD, focusing on cognitive deficits and the role of networks like the default mode network (DMN) and sensorimotor network (SMN).

Conclusions

Parkinson's Disease (PD) remains a complex and multifaceted neurodegenerative disorder, with its diagnosis and treatment posing significant challenges. The evolution of neuroimaging techniques over the past decades has markedly improved our understanding of PD, particularly in its early detection, differential diagnosis, and monitoring of disease progression.

Advanced MRI techniques like Voxel-Based Morphometry (VBM), Tensor-Based Morphometry (TBM), and cortical thickness measurements have significantly advanced our understanding of structural brain changes in Parkinson's disease (PD), helping differentiate it from similar conditions

like Multiple System Atrophy (MSA) and Progressive Supranuclear Palsy (PSP). Despite variability in findings due to patient differences, these methods, along with qMRI techniques like Quantitative Susceptibility Mapping (QSM) and Diffusion Tensor Imaging (DTI), have identified key biomarkers, such as iron overload in the substantia nigra, which are linked to disease severity and progression. Functional neuroimaging, including PET, SPECT, and fMRI, has further clarified the metabolic and functional abnormalities in PD, offering high sensitivity and specificity in diagnosis and providing insights into the cognitive deficits associated with the disease.

In conclusion, while significant progress has been made in the field of neuroimaging for PD, ongoing research is essential to refine these techniques and fully harness their potential in clinical practice. Despite these advancements, there is still no universally accepted imaging protocol for PD, highlighting the need for continued research and the development of standardized guidelines. The future of PD diagnosis and management lies in the continued exploration and integration of these advanced imaging modalities, which will undoubtedly contribute to a deeper understanding of the disease and the development of more effective therapeutic strategies.

References

Abós, A., Baggio, H. C., Segura, B., García-Díaz, A. I., Compta, Y., Martí, M. J., Valldeoriola, F., & Junqué, C. (2017). Discriminating cognitive status in Parkinson's disease through functional connectomics and machine learning. Scientific Reports, 7(1), 45347. https://doi.org/10.1038/srep45347

Amboni, M., Tessitore, A., Esposito, F., Santangelo, G., Picillo, M., Vitale, C., Giordano, A., Erro, R., de Micco, R., Corbo, D., Tedeschi, G., & Barone, P. (2015). Resting-state functional connectivity associated with mild cognitive impairment in Parkinson's disease. Journal of Neurology, 262(2), 425–434. https://doi.org/10.1007/s00415-014-7591-5

Andica, C., Kamagata, K., Hatano, T., Saito, A., Uchida, W., Ogawa, T., Takeshige-Amano, H., Zalesky, A., Wada, A., Suzuki, M., Hagiwara, A., Irie, R., Hori, M., Kumamaru, K. K., Oyama, G., Shimo, Y., Umemura, A., Pantelis, C., Hattori, N., & Aoki, S. (2019). Free-Water Imaging in White and Gray Matter in Parkinson's Disease. Cells, 8(8), 839. https://doi.org/10.3390/cells8080839

Andica, C., Kamagata, K., Hatano, T., Saito, Y., Uchida, W., Ogawa, T., Takeshige-Amano, H., Hagiwara, A., Murata, S., Oyama, G., Shimo, Y., Umemura, A., Akashi, T., Wada, A., Kumamaru, K. K., Hori, M., Hattori, N., & Aoki, S. (2020). Neurocognitive and psychiatric disorders-related axonal degeneration in Parkinson's disease. Journal of Neuroscience Research, 98(5), 936–949. https://doi.org/10.1002/jnr.24584

Ashburner, J., & Friston, K. J. (2000). Voxel-Based Morphometry—The Methods. NeuroImage, 11(6), 805–821. https://doi.org/10.1006/nimg.2000.0582

Azuma, M., Hirai, T., Yamada, K., Yamashita, S., Ando, Y., Tateishi, M., Iryo, Y., Yoneda, T., Kitajima, M., Wang, Y., & Yamashita, Y. (2016). Lateral Asymmetry and Spatial Difference of Iron Deposition in the Substantia Nigra of Patients with Parkinson Disease Measured with Quantitative Susceptibility Mapping. American Journal of Neuroradiology, 37(5), 782–788. https://doi.org/10.3174/ajnr.A4645

Baggio, H., Segura, B., Sala-Llonch, R., Marti, M., Valldeoriola, F., Compta, Y., Tolosa, E., & Junqué, C. (2015). Cognitive impairment and resting-state network connectivity in Parkinson's disease. Human Brain Mapping, 36(1), 199–212. https://doi.org/10.1002/hbm.22622

Barbosa, J. H. O., Santos, A. C., Tumas, V., Liu, M., Zheng, W., Haacke, E. M., & Salmon, C. E. G. (2015). Quantifying brain iron deposition in patients with Parkinson's disease using quantitative susceptibility mapping, R2 and R2*. Magnetic Resonance Imaging, 33(5), 559–565. https://doi.org/10.1016/j.mri.2015.02.021

Bergsland, N., Zivadinov, R., Schweser, F., Hagemeier, J., Lichter, D., & Guttuso Jr., T. (2019). Ventral posterior substantia nigra iron increases over 3 years in Parkinson's disease. Movement Disorders, 34(7), 1006–1013. https://doi.org/10.1002/mds.27730

Burciu, R. G., Ofori, E., Archer, D. B., Wu, S. S., Pasternak, O., McFarland, N. R., Okun, M. S., & Vaillancourt, D. E. (2017). Progression marker of Parkinson's disease: A 4-year multi-site imaging study. Brain, 140(8), 2183–2192. https://doi.org/10.1093/brain/awx146

Campabadal, A., Uribe, C., Segura, B., Baggio, H. C., Abos, A., Garcia-Diaz, A. I., Marti, M. J., Valldeoriola, F., Compta, Y., Bargallo, N., & Junque, C. (2017). Brain correlates of progressive olfactory loss in Parkinson's disease. Parkinsonism & Related Disorders, 41, 44–50. https://doi.org/10.1016/j.parkreldis.2017.05.005

Chougar, L., Pyatigorskaya, N., Degos, B., Grabli, D., & Lehéricy, S. (2020). The Role of Magnetic Resonance Imaging for the Diagnosis of Atypical Parkinsonism. Frontiers in Neurology, 11. https://doi.org/10.3389/fneur.2020.00665

Coakeley, S., & Strafella, A. P. (2017). Imaging tau pathology in Parkinsonisms. Npj Parkinson's Disease, 3(1), 1–9. https://doi.org/10.1038/s41531-017-0023-3

Díez-Cirarda, M., Strafella, A. P., Kim, J., Peña, J., Ojeda, N., Cabrera-Zubizarreta, A., & Ibarretxe-Bilbao, N. (2018). Dynamic functional connectivity in Parkinson's disease patients with mild cognitive impairment and normal cognition. NeuroImage: Clinical, 17, 847–855. https://doi.org/10.1016/j.nicl.2017.12.013

Du, G., Lewis, M. M., Sica, C., He, L., Connor, J. R., Kong, L., Mailman, R. B., & Huang, X. (2018). Distinct progression pattern of susceptibility MRI in the substantia nigra of Parkinson's patients. Movement Disorders, 33(9), 1423–1431. https://doi.org/10.1002/mds.27318

Du, G., Liu, T., Lewis, M. M., Kong, L., Wang, Y., Connor, J., Mailman, R. B., & Huang, X. (2016). Quantitative susceptibility mapping of the midbrain in Parkinson's disease. Movement Disorders, 31(3), 317–324. https://doi.org/10.1002/mds.26417

Dusek, P., Dezortova, M., & Wuerfel, J. (2013). Chapter Nine—Imaging of Iron. In K. P. Bhatia & S. A. Schneider (Eds.), International Review of Neurobiology (Vol. 110, pp. 195–239). Academic Press. https://doi.org/10.1016/B978-0-12-410502-7.00010-7

Fischl, B., & Dale, A. M. (2000). Measuring the thickness of the human cerebral cortex from magnetic resonance images. Proceedings of the National Academy of Sciences, 97(20), 11050–11055. https://doi.org/10.1073/pnas.200033797

Garcia-Diaz, A. I., Segura, B., Baggio, H. C., Uribe, C., Campabadal, A., Abos, A., Marti, M. J., Valldeoriola, F., Compta, Y., Bargallo, N., & Junque, C. (2018). Cortical thinning correlates of changes in visuospatial and visuoperceptual performance in Parkinson's disease: A 4-year follow-up. Parkinsonism & Related Disorders, 46, 62–68. https://doi.org/10.1016/j.parkreldis.2017.11.003

Garnett, E. S., Firnau, G., & Nahmias, C. (1983). Dopamine visualized in the basal ganglia of living man. Nature, 305(5930), 137–138. https://doi.org/10.1038/305137a0

Gee, M., Dukart, J., Draganski, B., Martin, W. W., Emery, D., & Camicioli, R. (2017). Regional volumetric change in Parkinson's disease with cognitive decline. Journal of the Neurological Sciences, 373, 88–94. https://doi.org/10.1016/j.jns.2016.12.030

Goetz, C. G., Tilley, B. C., Shaftman, S. R., Stebbins, G. T., Fahn, S., Martinez-Martin, P., Poewe, W., Sampaio, C., Stern, M. B., Dodel, R., Dubois, B., Holloway, R., Jankovic, J., Kulisevsky, J., Lang, A. E., Lees, A., Leurgans, S., LeWitt, P. A., Nyenhuis, D., … LaPelle, N. (2008). Movement Disorder Society-sponsored revision of the Unified Parkinson's Disease Rating Scale (MDS-UPDRS): Scale presentation and clinimetric testing results. Movement Disorders, 23(15), 2129–2170. https://doi.org/10.1002/mds.22340

Golan, H., Volkov, O., & Shalom, E. (2022). Nuclear imaging in Parkinson's disease: The past, the present, and the future. Journal of the Neurological Sciences, 436, 120220. https://doi.org/10.1016/j.jns.2022.120220

Gramsch, C., Reuter, I., Kraff, O., Quick, H. H., Tanislav, C., Roessler, F., Deuschl, C., Forsting, M., & Schlamann, M. (2017). Nigrosome 1 visibility at susceptibility weighted 7T MRI—A dependable diagnostic marker for Parkinson's disease or merely an inconsistent, age-dependent imaging finding? PLOS ONE, 12(10), e0185489. https://doi.org/10.1371/journal.pone.0185489

Guan, X., Lancione, M., Ayton, S., Dusek, P., Langkammer, C., & Zhang, M. (2024). Neuroimaging of Parkinson's disease by quantitative susceptibility mapping. NeuroImage, 289, 120547. https://doi.org/10.1016/j.neuroimage.2024.120547

Guan, X.-J., Guo, T., Zhou, C., Gao, T., Wu, J.-J., Han, V., Cao, S., Wei, H.-J., Zhang, Y.-Y., Xuan, M., Gu, Q.-Q., Huang, P.-Y., Liu, C.-L., Pu, J.-L., Zhang, B.-R., Cui, F., Xu, X.-J., & Zhang, M.-M. (2022). A multiple-tissue-specific magnetic resonance imaging model for diagnosing Parkinson's disease: A brain radiomics study. Neural Regeneration Research, 17(12), 2743. https://doi.org/10.4103/1673-5374.339493

Guttuso Jr, T., Sirica, D., Tosun, D., Zivadinov, R., Pasternak, O., Weintraub, D., Baglio, F., & Bergsland, N. (2022). Thalamic Dorsomedial Nucleus Free Water Correlates with Cognitive Decline in Parkinson's Disease. Movement Disorders, 37(3), 490–501. https://doi.org/10.1002/mds.28886

Hanganu, A., Bedetti, C., Degroot, C., Mejia-Constain, B., Lafontaine, A.-L., Soland, V., Chouinard, S., Bruneau, M.-A., Mellah, S., Belleville, S., & Monchi, O. (2014). Mild cognitive impairment is linked with faster rate of cortical thinning in patients with Parkinson's disease longitudinally. Brain, 137(4), 1120–1129. https://doi.org/10.1093/brain/awu036

He, N., Huang, P., Ling, H., Langley, J., Liu, C., Ding, B., Huang, J., Xu, H., Zhang, Y., Zhang, Z., Hu, X., Chen, S., & Yan, F. (2017). Dentate nucleus iron deposition is a potential biomarker for tremor-dominant Parkinson's disease. NMR in Biomedicine, 30(4), e3554. https://doi.org/10.1002/nbm.3554

Hoehn, M. M., & Yahr, M. D. (1967). Parkinsonism: Onset, progression, and mortality. Neurology, 17(5), 427–427.

Ibarretxe-Bilbao, N., Ramirez-Ruiz, B., Junque, C., Marti, M. J., Valldeoriola, F., Bargallo, N., Juanes, S., & Tolosa, E. (2010). Differential progression of brain atrophy in Parkinson's disease with and without visual hallucinations. Journal of Neurology, Neurosurgery & Psychiatry, 81(6), 650–657. https://doi.org/10.1136/jnnp.2009.179655

Kalia, L. V., & Lang, A. E. (2015). Parkinson's disease. The Lancet, 386(9996), 896–912. https://doi.org/10.1016/S0140-6736(14)61393-3

Kang, J. J., Chen, Y., Xu, G. D., Bao, S. L., Wang, J., Ge, M., Shen, L. H., & Jia, Z. Z. (2022). Combining quantitative susceptibility mapping to radiomics in diagnosing Parkinson's disease and assessing cognitive impairment. European Radiology, 32(10), 6992–7003. https://doi.org/10.1007/s00330-022-08790-8

Kau, T., Hametner, S., Endmayr, V., Deistung, A., Prihoda, M., Haimburger, E., Menard, C., Haider, T., Höftberger, R., Robinson, S., Reichenbach, J. R., Lassmann, H., Traxler, H., Trattnig, S., & Grabner, G. (2019). Microvessels may Confound the "Swallow Tail Sign" in Normal Aged Midbrains: A Postmortem 7 T SW-MRI Study. Journal of Neuroimaging, 29(1), 65–69. https://doi.org/10.1111/jon.12576

Kehagia, A. A., Barker, R. A., & Robbins, T. W. (2012). Cognitive Impairment in Parkinson's Disease: The Dual Syndrome Hypothesis. Neurodegenerative Diseases, 11(2), 79–92. https://doi.org/10.1159/000341998

Klaffke, S., Kuhn, A. A., Plotkin, M., Amthauer, H., Harnack, D., Felix, R., & Kupsch, A. (2006). Dopamine transporters, D2 receptors, and glucose metabolism in corticobasal degeneration. Movement Disorders, 21(10), 1724–1727. https://doi.org/10.1002/mds.21004

Lang, S., Hanganu, A., Gan, L. S., Kibreab, M., Auclair-Ouellet, N., Alrazi, T., Ramezani, M., Cheetham, J., Hammer, T., Kathol, I., Sarna, J., & Monchi, O. (2019). Network basis of the dysexecutive and posterior cortical cognitive profiles in Parkinson's disease. Movement Disorders, 34(6), 893–902. https://doi.org/10.1002/mds.27674

Lehericy, S., Vaillancourt, D. E., Seppi, K., Monchi, O., Rektorova, I., Antonini, A., McKeown, M. J., Masellis, M., Berg, D., Rowe, J. B., Lewis, S. J. G., Williams-Gray, C. H., Tessitore, A., Siebner, H. R., & on behalf of the International Parkinson and Movement Disorder Society (IPMDS)-Neuroimaging Study Group. (2017). The role of high-field magnetic resonance imaging in parkinsonian disorders: Pushing the boundaries forward. Movement Disorders, 32(4), 510–525. https://doi.org/10.1002/mds.26968

Litvan, I., Goldman, J. G., Tröster, A. I., Schmand, B. A., Weintraub, D., Petersen, R. C., Mollenhauer, B., Adler, C. H., Marder, K., Williams-Gray, C. H., Aarsland, D., Kulisevsky, J., Rodriguez-Oroz, M. C., Burn, D. J., Barker, R. A., & Emre, M. (2012). Diagnostic criteria for mild cognitive impairment in Parkinson's disease: Movement Disorder Society Task Force guidelines. Movement Disorders, 27(3), 349–356. https://doi.org/10.1002/mds.24893

Liu, T., Spincemaille, P., de Rochefort, L., Kressler, B., & Wang, Y. (2009). Calculation of susceptibility through multiple orientation sampling (COSMOS): A method for conditioning the inverse problem from measured magnetic field map to susceptibility source image in MRI. Magnetic Resonance in Medicine, 61(1), 196–204. https://doi.org/10.1002/mrm.21828

Mahlknecht, P., Krismer, F., Poewe, W., & Seppi, K. (2017). Meta-analysis of dorsolateral nigral hyperintensity on magnetic resonance imaging as a marker for Parkinson's disease. Movement Disorders, 32(4), 619–623. https://doi.org/10.1002/mds.26932

Mak, E., Su, L., Williams, G. B., Firbank, M. J., Lawson, R. A., Yarnall, A. J., Duncan, G. W., Owen, A. M., Khoo, T. K., Brooks, D. J., Rowe, J. B., Barker, R. A., Burn, D. J., & O'Brien, J. T. (2015). Baseline and longitudinal grey matter changes in newly diagnosed Parkinson's disease: ICICLE-PD study. Brain, 138(10), 2974–2986. https://doi.org/10.1093/brain/awv211

Mena, A. M., & Strafella, A. P. (2022). Imaging pathological tau in atypical parkinsonisms: A review. Clinical Parkinsonism & Related Disorders, 7, 100155. https://doi.org/10.1016/j.prdoa.2022.100155

Möller, H. E., Bossoni, L., Connor, J. R., Crichton, R. R., Does, M. D., Ward, R. J., Zecca, L., Zucca, F. A., & Ronen, I. (2019). Iron, Myelin, and the Brain: Neuroimaging Meets Neurobiology. Trends in Neurosciences, 42(6), 384–401. https://doi.org/10.1016/j.tins.2019.03.009

Nasreddine, Z. S., Phillips, N. A., Bédirian, V., Charbonneau, S., Whitehead, V., Collin, I., Cummings, J. L., & Chertkow, H. (2005). The Montreal Cognitive Assessment, MoCA: A Brief Screening Tool For Mild Cognitive Impairment. Journal of the American Geriatrics Society, 53(4), 695–699. https://doi.org/10.1111/j.1532-5415.2005.53221.x

Nicastro, N., Garibotto, V., & Burkhard, P. R. (2018). The role of molecular imaging in assessing degenerative parkinsonism – an updated review. Swiss Medical Weekly, 148(1718), Article 1718. https://doi.org/10.4414/smw.2018.14621

Nürnberger, L., Gracien, R.-M., Hok, P., Hof, S.-M., Rüb, U., Steinmetz, H., Hilker, R., Klein, J. C., Deichmann, R., & Baudrexel, S. (2017). Longitudinal changes of cortical microstructure in Parkinson's disease assessed with T1 relaxometry. NeuroImage: Clinical, 13, 405–414. https://doi.org/10.1016/j.nicl.2016.12.025

Ogawa, T., Hatano, T., Kamagata, K., Andica, C., Takeshige-Amano, H., Uchida, W., Saito, Y., Shimo, Y., Oyama, G., Umemura, A., Iwamuro, H., Ito, M., Hori, M., Aoki, S., & Hattori, N. (2021). White matter alterations in Parkinson's disease with levodopa-induced dyskinesia. Parkinsonism & Related Disorders, 90, 8–14. https://doi.org/10.1016/j.parkreldis.2021.07.021

Pasternak, O., Sochen, N., Gur, Y., Intrator, N., & Assaf, Y. (2009). Free water elimination and mapping from diffusion MRI. Magnetic Resonance in Medicine, 62(3), 717–730. https://doi.org/10.1002/mrm.22055

Paviour, D. C., Price, S. L., Stevens, J. M., Lees, A. J., & Fox, N. C. (2005). Quantitative MRI measurement of superior cerebellar peduncle in progressive supranuclear palsy. Neurology, 64(4), 675–679. https://doi.org/10.1212/01.WNL.0000151854.85743.C7

Poewe, W., Seppi, K., Tanner, C. M., Halliday, G. M., Brundin, P., Volkmann, J., Schrag, A.-E., & Lang, A. E. (2017). Parkinson disease. Nature Reviews Disease Primers, 3(1), 1–21. https://doi.org/10.1038/nrdp.2017.13

Politis, M. (2014). Neuroimaging in Parkinson disease: From research setting to clinical practice. Nature Reviews Neurology, 10(12), 708–722. https://doi.org/10.1038/nrneurol.2014.205

Postuma, R. B., Berg, D., Stern, M., Poewe, W., Olanow, C. W., Oertel, W., Obeso, J., Marek, K., Litvan, I., Lang, A. E., Halliday, G., Goetz, C. G., Gasser, T., Dubois, B., Chan, P., Bloem, B. R., Adler, C. H., & Deuschl, G. (2015). MDS clinical diagnostic criteria for Parkinson's disease. Movement Disorders, 30(12), 1591–1601. https://doi.org/10.1002/mds.26424

Prasad, S., Saini, J., Yadav, R., & Pal, P. K. (2018). Motor asymmetry and neuromelanin imaging: Concordance in Parkinson's disease. Parkinsonism & Related Disorders, 53, 28–32. https://doi.org/10.1016/j.parkreldis.2018.04.022

Price, S., Paviour, D., Scahill, R., Stevens, J., Rossor, M., Lees, A., & Fox, N. (2004). Voxel-based morphometry detects patterns of atrophy that help differentiate progressive supranuclear palsy and Parkinson's disease. NeuroImage, 23(2), 663–669. https://doi.org/10.1016/j.neuroimage.2004.06.013

Schmidt, M. A., Engelhorn, T., Marxreiter, F., Winkler, J., Lang, S., Kloska, S., Goelitz, P., & Doerfler, A. (2017). Ultra high-field SWI of the substantia nigra at 7T: Reliability and consistency of the swallow-tail sign. BMC Neurology, 17(1), 194. https://doi.org/10.1186/s12883-017-0975-2

Schwarz, S. T., Abaei, M., Gontu, V., Morgan, P. S., Bajaj, N., & Auer, D. P. (2013). Diffusion tensor imaging of nigral degeneration in Parkinson's disease: A region-of-interest and voxel-based study at 3 T and systematic review with meta-analysis. NeuroImage: Clinical, 3, 481–488. https://doi.org/10.1016/j.nicl.2013.10.006

Schwarz, S. T., Afzal, M., Morgan, P. S., Bajaj, N., Gowland, P. A., & Auer, D. P. (2014). The 'Swallow Tail' Appearance of the Healthy Nigrosome – A New Accurate Test of Parkinson's Disease: A Case-Control and Retrospective Cross-Sectional MRI Study at 3T. PLOS ONE, 9(4), e93814. https://doi.org/10.1371/journal.pone.0093814

Schwarz, S. T., Xing, Y., Tomar, P., Bajaj, N., & Auer, D. P. (2017). In Vivo Assessment of Brainstem Depigmentation in Parkinson Disease: Potential as a Severity Marker for Multicenter Studies. Radiology, 283(3), 789–798. https://doi.org/10.1148/radiol.2016160662

Takahashi, H., Watanabe, Y., Tanaka, H., Mihara, M., Mochizuki, H., Liu, T., Wang, Y., & Tomiyama, N. (2018). Quantifying changes in nigrosomes using quantitative susceptibility mapping and neuromelanin imaging for the diagnosis of early-stage Parkinson's disease. British Journal of Radiology, 91(1086), 20180037. https://doi.org/10.1259/bjr.20180037

Tang, C. C., Poston, K. L., Eckert, T., Feigin, A., Frucht, S., Gudesblatt, M., Dhawan, V., Lesser, M., Vonsattel, J.-P., Fahn, S., & Eidelberg, D. (2010). Differential diagnosis of parkinsonism: A metabolic imaging study using pattern analysis. The Lancet Neurology, 9(2), 149–158. https://doi.org/10.1016/S1474-4422(10)70002-8

Taniguchi, D., Hatano, T., Kamagata, K., Okuzumi, A., Oji, Y., Mori, A., Hori, M., Aoki, S., & Hattori, N. (2018). Neuromelanin imaging and midbrain volumetry in progressive supranuclear palsy and Parkinson's disease. Movement Disorders, 33(9), 1488–1492. https://doi.org/10.1002/mds.27365

Tessa, C., Lucetti, C., Giannelli, M., Diciotti, S., Poletti, M., Danti, S., Baldacci, F., Vignali, C., Bonuccelli, U., Mascalchi, M., & Toschi, N. (2014). Progression of brain atrophy in the early stages of Parkinson's disease: A longitudinal tensor-based morphometry study in de novo patients without cognitive impairment. Human Brain Mapping, 35(8), 3932–3944. https://doi.org/10.1002/hbm.22449

Tessitore, A., Esposito, F., Vitale, C., Santangelo, G., Amboni, M., Russo, A., Corbo, D., Cirillo, G., Barone, P., & Tedeschi, G. (2012). Default-mode network connectivity in cognitively unimpaired patients with Parkinson disease. Neurology, 79(23), 2226–2232. https://doi.org/10.1212/WNL.0b013e31827689d6

Teune, L. K., Renken, R. J., Mudali, D., De Jong, B. M., Dierckx, R. A., Roerdink, J. B. T. M., & Leenders, K. L. (2013). Validation of parkinsonian disease-related metabolic brain patterns. Movement Disorders, 28(4), 547–551. https://doi.org/10.1002/mds.25361

Thobois, S., Prange, S., Scheiber, C., & Broussolle, E. (2019). What a neurologist should know about PET and SPECT functional imaging for parkinsonism: A practical perspective. Parkinsonism & Related Disorders, 59, 93–100. https://doi.org/10.1016/j.parkreldis.2018.08.016

Thomas, G. E. C., Hannaway, N., Zarkali, A., Shmueli, K., & Weil, R. S. (2024). Longitudinal Associations of Magnetic Susceptibility with Clinical Severity in Parkinson's Disease. Movement Disorders, 39(3), 546–559. https://doi.org/10.1002/mds.29702

Thomas, G. E. C., Leyland, L. A., Schrag, A.-E., Lees, A. J., Acosta-Cabronero, J., & Weil, R. S. (2020). Brain iron deposition is linked with cognitive severity in Parkinson's disease. Journal of Neurology, Neurosurgery & Psychiatry, 91(4), 418–425. https://doi.org/10.1136/jnnp-2019-322042

Wu, T., Long, X., Wang, L., Hallett, M., Zang, Y., Li, K., & Chan, P. (2011). Functional connectivity of cortical motor areas in the resting state in Parkinson's disease. Human Brain Mapping, 32(9), 1443–1457. https://doi.org/10.1002/hbm.21118

Wu, T., Wang, L., Chen, Y., Zhao, C., Li, K., & Chan, P. (2009). Changes of functional connectivity of the motor network in the resting state in Parkinson's disease. Neuroscience Letters, 460(1), 6–10. https://doi.org/10.1016/j.neulet.2009.05.046

Xing, Y., Sapuan, A., Dineen, R. A., & Auer, D. P. (2018). Life span pigmentation changes of the substantia nigra detected by neuromelanin-sensitive MRI. Movement Disorders, 33(11), 1792–1799. https://doi.org/10.1002/mds.27502

Yang, J., Burciu, R. G., & Vaillancourt, D. E. (2018). Longitudinal Progression Markers of Parkinson's Disease: Current View on Structural Imaging. Current Neurology and Neuroscience Reports, 18(12), 83. https://doi.org/10.1007/s11910-018-0894-7

Yau, Y., Zeighami, Y., Baker, T. E., Larcher, K., Vainik, U., Dadar, M., Fonov, V. S., Hagmann, P., Griffa, A., Mišić, B., Collins, D. L., & Dagher, A. (2018). Network connectivity determines cortical thinning in early Parkinson's disease progression. Nature Communications, 9(1), 12. https://doi.org/10.1038/s41467-017-02416-0

Zeng, Q., Guan, X., Law Yan Lun, J. C. F., Shen, Z., Guo, T., Xuan, M., Gu, Q., Xu, X., Chen, M., & Zhang, M. (2017). Longitudinal Alterations of Local Spontaneous Brain Activity in Parkinson's Disease. Neuroscience Bulletin, 33(5), 501–509. https://doi.org/10.1007/s12264-017-0171-9

Zhang, Y., Huang, P., Wang, X., Xu, Q., Liu, Y., Jin, Z., Li, Y., Cheng, Z., Tang, R., Chen, S., He, N., Yan, F., & Haacke, E. M. (2023). Visualizing the deep cerebellar nuclei using quantitative susceptibility mapping: An application in healthy controls, Parkinson's disease patients and essential tremor patients. Human Brain Mapping, 44(4), 1810–1824. https://doi.org/10.1002/hbm.26178

Zhang, Y., Yang, M., Wang, F., Chen, Y., Liu, R., Zhang, Z., & Jiang, Z. (2022). Histogram Analysis of Quantitative Susceptibility Mapping for the Diagnosis of Parkinson's Disease. Academic Radiology, 29, S71–S79. https://doi.org/10.1016/j.acra.2020.10.027

QMENTA®

IMAGING TO INSIGHT

LEARN MORE

US Headquarters

75 State Street, Suite 100
Boston, MA 02109
+1 339 368 8040

EU Offices

C/ Roger de Llúria 46, Pral. 1ª
08009 Barcelona, Spain
+34 933 282 007

qmenta_inc

@QMENTA_Inc

www.qmenta.com